COUPLING OF EXTENDED BML MODEL AND ADVANCED TURBULENCE AND MIXING MODELS IN PREDICTING PARTIALLY PREMIXED FLAMES

A. Maltsev, A. Sadiki and J. Janicka
Institute of Energy and Power Plant Technology,
Darmstadt University of Technology
Petersenstr. 30, 64287 Darmstadt, Germany
maltsev@hrzpub.tu-darmstadt.de, sadiki@ekt.tu-darmstadt.de, janicka@ekt.tu-darmstadt.de

ABSTRACT

In this work we present a complete model for the description of partially premixed turbulent flames in technically relevant combustion regimes. These flames are the most commonly encountered in engineering applications. The closure is based on the extension of the well-known Bray-Moss-Libby model. In fact, the BML model is coupled to the mixing transport model providing variable equivalence ratio that distinguishes partially premixed flames. Simple equilibrium chemistry model describes the expansion ratio and species formation conditioned on the flame front. A presumed PDF approach is used for the turbulence-chemistry interaction treatment. Two main aspects are investigated: (i) An algebraic closure for the mean reaction rate in the single reactive scalar transport equation is formulated based on the flame surface density approach and on the assumption that the flame surface has a fractal character. The influence of the fractal dimension in the model is estimated. (ii) Two levels of complexity of turbulence models are employed in order to examine the importance of the second moment turbulence closure in the presented approach. Redistribution terms in second moment transport equations are extended to take into account strongly variable density effects. These submodels are then combined in various complete models and assessed simulating piloted partially premixed flame. The results obtained with the complete second order closures for the velocity and single reactive scalar correlations show the best agreement with experimental data for flow properties and species distributions.

INTRODUCTION

Turbulent partially premixed flames take place in a huge amount of technical devices and applications such as internal combustion engines, modern gas turbine combustors etc. The importance of their fundamental understanding as well as possible prediction is difficult to underestimate. The main feature differing them from pure diffusion and pure premixed flames is that both mixing and flame propagation processes play a significant role controlling the whole system. The most modelling efforts during the last time have been undertaken in investigations of turbulent diffusion flames. The attention of researchers to premixed flames was limited to some idealized one-dimensional configurations where an attempt was made to provide a closure for the turbulent flame speed. It has resulted in a number of "one flame" models being of small use in practical engineering computations.

Thus the objective of this work is the development and assessment of a complete model for the description of partially premixed turbulent flames in technically relevant combustion regimes. Several modelling approaches were proposed in the last decades for the description of turbulent premixed flames (Bray 1994, Peters 2000). Containing a great potential in application to LES or DNS context the so called G-equation model (see Peters 2000) requires enormous computational efforts due to its coupling to a level-set method. Furthermore an advantage of this approach in RANS context is not obvious. The single reactive scalar approach or well-known Bray-Moss-Libby model (Bray et al. 1994) is implied in the present work in conjunction with mixing transport in order to provide variable equivalence ratio. Several modelling aspects such as velocity and scalar turbulence modelling and application of fractal theory to an algebraic closuring of the flame surface density are presented and discussed in the next sections. The resulting model is further assessed. Predictions of flow properties and species distribution are provided for the partially premixed methane/air jet flame at two different Reynolds numbers experimentally investigated by Chen et al. (1996).

MODELLING APPROACH

Mean flow and scalar field

Assuming thermochemically constant pressure the incompressible variable density Favre averaged continuity and Navier-Stokes equations are applied for the description of the mean flow field. Neglecting viscous terms at high Reynolds number they are given by

$$\frac{\partial \overline{\rho}}{\partial t} + \frac{\partial}{\partial x_i}(\overline{\rho}\widetilde{u}_i) = 0 \tag{1}$$

$$\frac{\partial \overline{\rho}\widetilde{u}_i}{\partial t} + \frac{\partial}{\partial x_j}(\overline{\rho}\widetilde{u}_j\widetilde{u}_i) = -\frac{\partial \overline{P}}{\partial x_i} + \frac{\partial}{\partial x_j}\left(-\overline{\rho}\widetilde{u_j''u_i''}\right) \tag{2}$$

The modelling of the unclosed Reynolds stresses is postponed to the next section. The thermochemistry is described by means of the single reactive scalar defined as a dimensionless temperature:

$$c = \frac{T - T_u}{T_b - T_u} \tag{3}$$

where subscripts "u" and "b" correspond to unburned and burned flame side, respectively. The influence of the heat loss due to the radiation on the flow properties is assumed to be negligible that is also the case for the considered non-confined flames. For a given expansion ratio

$$\tau = \frac{T_b - T_u}{T_u} \tag{4}$$

using infinitely thin flame surface assumption (Bray et al. 1994) resulting in a bimodal PDF for c an algebraic relation

for the mean density can be derived:

$$\overline{\rho} = \frac{\rho_u}{1+\tau\widetilde{c}} \tag{5}$$

A Favre averaged transport equation for the single reactive scalar is given by:

$$\frac{\partial\overline{\rho}\widetilde{c}}{\partial t} + \frac{\partial}{\partial x_j}(\overline{\rho}\widetilde{u}_j\widetilde{c}) = \frac{\partial}{\partial x_j}\left(-\overline{\rho}\widetilde{c''u''_j}\right) + \overline{S_c} \tag{6}$$

where $\overline{S_c}$ is the mean reaction rate. To extend this model to the partially premixed combustion, we account for the changes in equivalence ratio appearing in partially premixed flames by introducing an additional conservative scalar, the mixture fraction ξ. The expansion ratio τ varies with the equivalence ratio ϕ which in turn can be directly related to the mixture fraction $\tau = \tau(\xi)$. Expansion ratio in expression (4) is calculated from the adiabatic flame temperature T_b using an assumption of chemical equilibrium. Similarly to the adiabatic flame temperature the chemical equilibrium values for different mixture fractions can be taken for the stable combustion products' concentrations. This approach is usually followed in case of a pure diffusion flame. To extend it to the partially premixed flame the mass fractions of combustion products $X^b_\alpha(\xi)$ taken under condition of being on the burnt side of the flame front must be multiplied by the probability p^b of being behind the flame front:

$$X_\alpha(\xi, p^b) = X^b_\alpha(\xi)p^b \tag{7}$$

In our case this probability can be directly related to the single reactive scalar $p^b = c$. So that

$$X_\alpha(\xi, p^b) = X^b_\alpha(\xi)c \tag{8}$$

In order to account for the strongly non-linear turbulent-chemistry interaction a presumed PDF approach is introduced. The PDF is assumed to have a form of a beta-function constructed from the mean and variance of the mixture fraction. The mean values of the expansion ratio $\overline{\tau}$ and "burned" mass fractions $\widetilde{X^b_\alpha}$ are thus obtained from the PDF integration:

$$\overline{\tau}(\widetilde{\xi}, \widetilde{\xi''^2}) = \int_0^1 \tau(\xi)P_\beta(\widetilde{\xi}, \widetilde{\xi''^2})d\xi \tag{9}$$

$$\widetilde{X^b_\alpha}(\widetilde{\xi}, \widetilde{\xi''^2}) = \frac{1}{\overline{\rho}}\int_0^1 \rho(\xi)X^b_\alpha(\xi)P_\beta(\widetilde{\xi}, \widetilde{\xi''^2})d\xi \tag{10}$$

Again assuming a bimodal PDF of c (Bray et al. 1994) one can show that

$$\widetilde{X_\alpha}(\widetilde{c}, \widetilde{\xi}, \widetilde{\xi''^2}) = \widetilde{c}\widetilde{X^b_\alpha}(\widetilde{\xi}, \widetilde{\xi''^2}) \tag{11}$$

The dependencies $\overline{\tau}(\widetilde{\xi}, \widetilde{\xi''^2})$ and $\widetilde{X^b_\alpha}(\widetilde{\xi}, \widetilde{\xi''^2})$ are stored in a look-up table that is interpolated during the calculations. For the mean mixture fraction $\widetilde{\xi}$ and its variance $\widetilde{\xi''^2}$ the following transport equations have to be solved:

$$\frac{\partial\overline{\rho}\widetilde{\xi}}{\partial t} + \frac{\partial}{\partial x_j}(\overline{\rho}\widetilde{u}_j\widetilde{\xi}) = \frac{\partial}{\partial x_j}\left(-\overline{\rho}\widetilde{\xi''u''_j}\right) \tag{12}$$

$$\frac{\partial\overline{\rho}\widetilde{\xi''^2}}{\partial t} + \frac{\partial}{\partial x_j}(\overline{\rho}\widetilde{u}_j\widetilde{\xi''^2}) = \frac{\partial}{\partial x_j}\left(-\overline{\rho}\widetilde{u''_j\xi''^2}\right) - 2\overline{\rho}\widetilde{u''_j\xi''}\frac{\partial\widetilde{f}}{\partial x_j} - 2\frac{\mu}{Sc}\overline{\frac{\partial\xi''}{\partial x_j}\frac{\partial\xi''}{\partial x_j}} \tag{13}$$

Though more complex and sophisticated in terms of chemical kinetics models for the species formation can be applied (see Maltsev et al. 2003). It is, however, not the main focus of the present work. The correlations appearing from the averaging in (2),(6),(12) and (13) as well as mean reaction rate in (6) need to be closed. This is the topic of the next sections.

Velocity and scalar turbulence closure

The unclosed Reynolds-stress correlations in (2) and scalar fluxes in (6) and (12) are closed, first, using simple Boussinesq

$$-\overline{\rho}\widetilde{u''_j u''_i} = \mu_t\left(\frac{\partial\widetilde{u}_i}{\partial x_j} + \frac{\partial\widetilde{u}_j}{\partial x_i}\right) - \frac{2}{3}\overline{\rho}k\delta_{ij} \tag{14}$$

and gradient diffusion hypothesis

$$-\overline{\rho}\widetilde{\psi''u''_i} = \frac{\mu_t}{\sigma_\psi}\frac{\partial\widetilde{\psi}}{\partial x_i} \tag{15}$$

Here ψ corresponds to a general scalar and σ_ψ to its turbulent Schmidt number. $k = \frac{1}{2}\widetilde{u''_i u''_i}$ is the turbulent kinetic energy and $\mu_t = C_\mu\overline{\rho}\frac{k^2}{\varepsilon}$ - turbulent viscosity. For the determination of μ_t a linear $k-\varepsilon$ model (Jones & Launder 1972) is here applied. The transport equation for k and ε solved are

$$\frac{\partial\overline{\rho}k}{\partial t} + \frac{\partial}{\partial x_k}(\widetilde{u}_k\overline{\rho}k) = \frac{\partial}{\partial x_k}\left(\frac{\mu_t}{\sigma_k}\frac{\partial k}{\partial x_k}\right) - \overline{\rho}\widetilde{u''_i u''_j}\frac{\partial\widetilde{u}_i}{\partial x_j} - \overline{\rho}\varepsilon - \overline{u''_k}\frac{\partial\overline{P}}{\partial x_k} \tag{16}$$

$$\frac{\partial\overline{\rho}\varepsilon}{\partial t} + \frac{\partial}{\partial x_k}(\widetilde{u}_k\overline{\rho}\varepsilon) = \frac{\partial}{\partial x_k}\left(\frac{\mu_t}{\sigma_k}\frac{\partial\varepsilon}{\partial x_k}\right) - \overline{\rho}C_{\varepsilon 1}\frac{\varepsilon}{k}\overline{u''_i u''_j}\frac{\partial\widetilde{u}_i}{\partial x_j} - \overline{\rho}C_{\varepsilon 2}\frac{\varepsilon^2}{k} - C_{\varepsilon 3}\frac{\varepsilon}{k}\overline{u''_k}\frac{\partial\overline{P}}{\partial x_k} \tag{17}$$

where $\overline{P} = p - p'$ is the mean pressure. Secondly, a complete second moment closure (SMC) with six additional Reynolds stress transport equations[1]

$$\frac{\partial\overline{\rho}\widetilde{u''_i u''_j}}{\partial t} + \frac{\partial}{\partial x_k}(\widetilde{u}_k\overline{\rho}\widetilde{u''_i u''_j}) = \underbrace{-\overline{\rho}\left(\widetilde{u''_i u''_k}\frac{\partial\widetilde{u}_j}{\partial x_k} + \widetilde{u''_j u''_k}\frac{\partial\widetilde{u}_i}{\partial x_k}\right) + \frac{\partial}{\partial x_k}\left(-\overline{\rho}\widetilde{u''_i u''_j u''_k} - \frac{2}{3}\overline{p'u''_k}\delta_{ij}\right)}_{T_{ijk}} \underbrace{-\left(\tau''_{jk}\frac{\partial u''_i}{\partial x_k} + \tau''_{ik}\frac{\partial u''_j}{\partial x_k}\right)}_{\overline{\rho}\varepsilon_{ij}} \underbrace{-\left(\overline{u''_i\frac{\partial p'}{\partial x_j}} + \overline{u''_j\frac{\partial p'}{\partial x_i}} - \frac{2}{3}\overline{u''_k\frac{\partial p'}{\partial x_k}}\delta_{ij}\right)}_{\phi^R_{ij}} \underbrace{-\left(\overline{u''_i}\frac{\partial\overline{P}}{\partial x_j} + \overline{u''_j}\frac{\partial\overline{P}}{\partial x_i}\right)}_{\Phi_{ij}} \tag{18}$$

[1]Here the pressure dilatation term is neglected

and three scalar flux transport equations for the single reactive scalar / velocity correlation vector

$$\begin{aligned}
&\frac{\partial \overline{\rho} \widetilde{c'' u_j''}}{\partial t} + \frac{\partial}{\partial x_k}(\widetilde{u}_k \overline{\rho} \widetilde{c'' u_j''}) = \\
&- \overline{\rho}\left(\widetilde{u_k'' c''} \frac{\partial \widetilde{u_j}}{\partial x_k} + \widetilde{u_k'' u_j''} \frac{\partial \widetilde{c}}{\partial x_k} \right) \\
&\underbrace{+ \frac{\partial}{\partial x_k}\left(- \overline{\rho} \widetilde{u_j'' u_k'' c''} \right) - \frac{\partial}{\partial x_j}(\overline{p' c''})}_{T_{jkc}} \\
&\underbrace{- \left(\overline{\tau_{jk}'' \frac{\partial c''}{\partial x_k}} - \overline{j_k'' \frac{\partial u_j''}{\partial x_k}} \right)}_{\overline{\rho} \varepsilon_{cj}} \\
&\underbrace{+ \overline{p' \frac{\partial c''}{\partial x_j}}}_{\phi_{jc}^S} \underbrace{- \overline{c''} \frac{\partial \overline{P}}{\partial x_j}}_{\Phi_{jc}} + \overline{u_j'' S_c}
\end{aligned} \tag{19}$$

are used. For the turbulent transport terms in (18) and (19) the simple isotropic model of Shir (1973) is employed

$$T_{ijk} = \frac{\partial}{\partial x_k}\left(C_S \overline{\rho} \frac{k^2}{\varepsilon} \frac{\partial \widetilde{u_i'' u_j''}}{\partial x_k} \right) \tag{20}$$

$$T_{jkc} = \frac{\partial}{\partial x_k}\left(C_S \overline{\rho} \frac{k^2}{\varepsilon} \frac{\partial \widetilde{c'' u_j''}}{\partial x_k} \right) \tag{21}$$

Dissipation term in (18) is modelled by assuming a local isotropy of the small scales

$$\varepsilon_{ij} = \frac{2}{3} \varepsilon \delta_{ij} \tag{22}$$

Similarly to equation (17) the following ε equation in its modelled form has to be solved[2]:

$$\begin{aligned}
&\frac{\partial \overline{\rho} \varepsilon}{\partial t} + \frac{\partial}{\partial x_j}(\overline{\rho} \widetilde{u}_j \varepsilon) = \frac{\partial}{\partial x_j}\left(C_S \overline{\rho} \frac{k^2}{\varepsilon} \frac{\partial \varepsilon}{\partial x_j} \right) \\
&- C_{\varepsilon 1} \overline{\rho} \frac{\varepsilon}{k} \widetilde{u_j'' u_i''} \frac{\partial \widetilde{u}_i}{\partial x_j} - C_{\varepsilon 2} \overline{\rho} \frac{\varepsilon^2}{k} - C_{\varepsilon 3} \frac{\varepsilon}{k} \overline{u_l''} \frac{\partial \overline{P}}{\partial x_l}
\end{aligned} \tag{23}$$

According to the BML theory the exact expressions for the Reynolds averaged Favre fluctuations of velocity and single reactive scalar appearing in (16)-(23) (preferential acceleration terms Φ_{ij}, Φ_{jc}):

$$\overline{u_i''} = \tau \frac{\overline{\rho}}{\rho_u} \widetilde{u_i'' c''}, \; \overline{c''} = \tau \frac{\overline{\rho}}{\rho_u} \widetilde{c''^2} \tag{24}$$

with

$$\widetilde{c''^2} = \widetilde{c}(1 - \widetilde{c}) \tag{25}$$

can be derived. To close the redistribution term in (18), ϕ_{ij}^R, and scrambling term in (19), ϕ_{jc}^S, following Lindstedt et al. (1999) an extension to the constant density redistribution models with additional terms comprising a preferential acceleration part is used here in conjunction with linear redistribution models for the Reynolds stress (Launder et al. 1976) and scalar flux (Launder et al. 1979). Modelled form of redistribution terms is thus given by the sum of a constant density part (superscript "CD") and a preferential acceleration part (superscript "A"):

$$\phi_{ij}^R = \phi_{ij}^{CD} + \phi_{ij}^A \tag{26}$$

[2]Here again the model of Shir is applied for the turbulent transport

Table 1: Model constants

σ_ψ	σ_k	σ_ε	C_μ	C_S	$C_{\varepsilon 1}$	$C_{\varepsilon 2}$	$C_{\varepsilon 3}$
0.7	1.0	1.3	0.09	0.1	1.44	1.9	1.44
C_1	C_2	C_3	C_4	C_1^S	C_2^S	C_{A_R}	C_{A_S}
1.5	-0.58	0.764	-0.18	3.0	0.33	-1/3	-0.3

$$\phi_{jc}^S = \phi_{jc}^{CD} + \phi_{jc}^A \tag{27}$$

The constant density parts are given by

$$\begin{aligned}
\phi_{ij}^{CD} = \overline{\rho}\Bigg[&- C_1 \varepsilon \left(\frac{\widetilde{u_i'' u_j''}}{k} - \frac{2}{3}\delta_{ij} \right) + C_2 \widetilde{u_k'' u_l''} \frac{\partial \widetilde{u_k}}{\partial x_l} \delta_{ij} \\
&- C_3 \left(\widetilde{u_i'' u_k''} \frac{\partial \widetilde{u}_j}{\partial x_k} + \widetilde{u_j'' u_k''} \frac{\partial \widetilde{u}_i}{\partial x_k} \right) + C_4 k \left(\frac{\partial \widetilde{u}_i}{\partial x_j} + \frac{\partial \widetilde{u_j}}{\partial x_i} \right) \\
&- \left(\frac{3}{2} C_2 + C_3 \right) \left(\widetilde{u_k'' u_j''} \frac{\partial \widetilde{u}_k}{\partial x_i} + \widetilde{u_k'' u_i''} \frac{\partial \widetilde{u}_k}{\partial x_j} \right) \Bigg]
\end{aligned} \tag{28}$$

$$\phi_{jc}^{CD} = \overline{\rho}\left(- C_1^S \frac{\varepsilon}{k} \widetilde{u_j'' c''} + C_2^S \widetilde{u_i'' c''} \frac{\partial \widetilde{u_j}}{\partial x_i} \right) \tag{29}$$

while the preferential acceleration parts are expressed as:

$$\phi_{ij}^A = C_{A_R}\left(\Phi_{ij} - \frac{1}{3}\delta_{ij}\Phi_{kk} \right) \tag{30}$$

$$\phi_{jc}^A = C_{A_S} \Phi_{jc} \tag{31}$$

The modelled dissipation term and chemical correlation term in (19) are combined in one modelling expression:

$$-\overline{\rho} \varepsilon_{cj} + \overline{u_j'' S_c} = \frac{\overline{S_c}}{\widetilde{c''^2}} \left(\frac{1}{2} - \widetilde{c} \right) \widetilde{u_j'' c''} \tag{32}$$

All the model constant values used can be found in table 1.

The unclosed turbulent flux in (13) is modelled both in the case of $k - \varepsilon$ and SMC models by means of the gradient diffusion hypothesis:

$$-\overline{\rho} \widetilde{u_j'' \xi''^2} = \frac{\mu_t}{\sigma_\phi} \frac{\partial \widetilde{\xi''^2}}{\partial x_j} \tag{33}$$

The dissipation term in (13) is approximated through the inverse integral turbulent time scale:

$$2 \frac{\mu}{Sc} \overline{\frac{\partial \xi''}{\partial x_j} \frac{\partial \xi''}{\partial x_j}} = 2 \overline{\rho} \frac{\varepsilon}{k} \widetilde{\xi''^2} \tag{34}$$

Mean reaction rate closure

We use the flame surface density approach to approximate the mean rate of formation of the single reactive scalar. In this approach the mean rate of formation is given by a product of unburned density ρ_u, laminar burning velocity u_L^0, that depends on the mixture fraction in partially premixed flames, and the flame surface density Σ:

$$\overline{S_c} = \rho_u \overline{u_L^0} \Sigma \tag{35}$$

In this work the laminar burning velocity was obtained by fitting the experimental data of Law (1993) for methane/air combustion system. Stretching is not considered here, since such ad-hoc formulations always lack generality and just

introduce an additional uncertainties. Therefore, the unstrained laminar value of u_L^0 is directly used in (35). Similarly to the expansion ratio, the functional dependency $u_L^0(\xi)$ from the data of Law (1993) is pre-integrated according to (9) and the mean value of $\widetilde{u_L^0}(\widetilde{\xi}, \widetilde{\xi''^2})$, stored in a look-up table, used in computations.

The modelling of the flame surface density, that measures the flame front convolutions, is the most crucial aspect of the present model. An exact balance equation can be derived for this quantity. This equation, however, contains lots of unclosed terms which modelling requires an empirical input. The model used here is that based on the assumption that the flame surface has a fractal character (Gouldin 1987) with inner cut-off to be equal the Kolmogorov scale η and outer cut-off to be equal the turbulent integral length scale l_t. This results in an algebraic closure:

$$\Sigma = \frac{1}{l_t}\left(\frac{l_t}{\eta}\right)^{D-2} \tag{36}$$

with D being a fractal dimension. D must be between 2 and 3: theoretical analysis of Mandelbrot (1975) suggests two boundary values $2\frac{1}{3}$ and $2\frac{2}{3}$; experimental investigations of Sreenivasan et al. (1986) in turbulent shear flows show that constant property surfaces in these flows are fractal with D between 2.35 and about 2.6. Substitution of expressions for the length scales

$$l_t = C_L\frac{k^{3/2}}{\varepsilon}, \quad \eta = \frac{\nu^{3/4}}{\varepsilon^{1/4}} \tag{37}$$

into expression (36) yields

$$\Sigma = \left(C_L\frac{k^{3/2}}{\varepsilon}\right)^{D-3}\left(\frac{\nu^{3/4}}{\varepsilon^{1/4}}\right)^{2-D} \tag{38}$$

Expression (38) is true if the flame surface is distributed randomly in a given volume or if the probability of finding flamelet in given volume is equal unity. From the BML theory this probability is equal to $\widetilde{c}(1-\widetilde{c})$ and the final expression for the mean reaction rate is

$$\overline{\dot{S}_c} = \rho_u\,\widetilde{u_L^0}\left(C_L\frac{k^{3/2}}{\varepsilon}\right)^{D-3}\left(\frac{\nu^{3/4}}{\varepsilon^{1/4}}\right)^{2-D}\widetilde{c}(1-\widetilde{c}) \tag{39}$$

The scaling constant C_L in (37) was found to depend on the Reynolds number Re_λ based on the Taylor length scale λ. The scattering of a big number of experimental data on the decay of isotropic turbulence in the study of Sreenivasan (1984) shows the constant C_L to asymptotically approach the value $C_L = 0.41$ as $Re_\lambda \geq 50$. Assuming the Reynolds number sufficiently large this value is also used in the present work. Lindstedt et al. (1999) assumes the fractal dimension to be $D = 7/3$ (the lower boundary suggested by Mandelbrot 1975) resulting in an elegant model for the flame surface density

$$\Sigma = C_R\frac{1}{(\nu\varepsilon)^{1/4}}\frac{\varepsilon}{k} \tag{40}$$

with C_R to be a constant of order of unity. But this parameter had to be tuned to $C_R = 2.6$ in the work of Lindstedt et al. (1999) in order to reproduce the measurements in a counter flow premixed flame configuration. That is why this practice is not followed here. We believe that rather the fractal dimension D should be a free parameter. This parameter should depend on the turbulent Reynolds number that is clearly demonstrated by our simulation results.

NUMERICAL PROCEDURE

The governing equations were integrated in the three-dimensional CFD code FASTEST-3D. The program features a finite volume based, geometry flexible code for the block-structured, non-orthogonal grids with SIMPLE similar implicit velocity pressure coupling procedure. A TVD based discretization scheme with automatical flux blending is applied to convective fluxes and central differences scheme to diffusion fluxes in momentum and scalar transport equations. Thus the optimal suppression of numerical diffusion is achieved while avoiding oscillations and proving high convergence rate. The test cases investigated here are two-dimensional (axisymmetric) and statistically steady. Thus a computational domain consisting of a 15 degree sector with symmetry boundary conditions in tangential direction is sufficient for the simulation. Unsteady terms are neglected and the whole equation system is underrelaxated until a steady state solution is achieved.

INVESTIGATED CONFIGURATIONS, GRID AND BOUNDARY CONDITIONS

Two stoichiometrically premixed piloted methane/air jet flames at different Reynolds numbers experimentally investigated by Chen et al. (1996) are simulated for the assessment of the whole model. Three configurations with different Reynolds numbers were measured by Chen et al. (1996) in order to have a comprehensive data basis for different combustion regimes appearing in the combustion classification diagram by Peters (2000). In the present work the flame configurations "F2" and "F3" are investigated. The main features of these flames are: Reynolds number $Re = 40000$ for "F2" and $Re = 24000$ for "F3" flame, jet diameter $D = 0.012\ m$, jet bulk velocity $U_0 = 50\ m/s$ for "F2" and $U_0 = 30\ m/s$ for "F3" flame, pilot bulk velocity $U_p = 0.22\ m/s$. Both jet and pilot flow are stoichiometrically premixed. LDA measurements of velocity field as well as scalar and temperature measurements with Rayleigh thermometry and Raman/Reyleigh LIPF-OH techniques were provided up to $x/D = 8.5$ in "F3" and up to $x/D = 10.5$ in "F2" flame. According to the estimations of Chen et al. (1996) both these two flames are located in the technically relevant distributed reaction zone in combustion diagram. In this zone the Kolmogorov scale η is still less than the reaction zone thickness and , thus, the thin flame surface assumption used in the BML theory is applicable. The flames were simulated using axisymmetrical two-dimensional grid with computational domain of $80D$x$30D$ discretized with 100x80 cells in axial and radial direction respectively. The inflow data for mean velocity and turbulent quantities were taken from LDA measurements of Chen et al. (1996). The inflow dissipation rate ε was defined using empirical relation $\varepsilon = k^{3/2}/l_t$ with constant turbulent length scale $l_t = 0.002m$. For the mixture fraction, the stoichiometric value $f_{st} = 0.055$ was specified at the jet and pilot inflow. The value of $\widetilde{c}$ was taken to be zero (unburnt) on the nozzle exit and unity (burnt) at the pilot flame.

RESULTS AND DISCUSSION

Using the same combustion model, numerical calculations with complete second order moment closures for velocity and scalar fields as well as with the standard $k-\varepsilon$ model combined with gradient diffusion transport for the single reactive scalar were performed. The free parameter in the mean reaction rate model (39), fractal dimension D,

was set to the value of $D = 7.3/3$ in "F3" and $D = 7.5/3$ in "F2" flame. With these values the best agreement with experimental data could be achieved. It should be noted that these numbers surprisely locate within the theoretically postulated (Mandelbrot 1975) and experimentally observed (Sreenivasan 1886) boundaries, approximately $D = 7/3$ and $D = 8/3$. This fact confirms a suggestion that the fractal dimension should be a function of the Reynolds number because only the Reynolds number varies in these two flames. Unfortunately no systematical experimental investigations exist on this subject. Though it would be a great advantage and could significantly generalize the presented model formulation. The simulation results are presented in Fig. 1-10. The quantities are plotted along the radial direction at axial position $x/D = 8.5$ for the flame"F3" (left) and at $x/D = 10.5$ for the flame "F2" (right). These are the latest downstream position provided by the measurements. Fig. 1 and 2 show good reproduction of the mean axial velocity with small superiority of the SMC though the differences to the experimental data for the flame "F3" are bigger. It slightly contrasts, however, with the prediction of the mean single reactive scalar (Fig. 3 and 4) where in both two configurations an excellent agreement is achieved with the SMC while the $k-\varepsilon$ based model clearly fails particularly in "F2" case. The agreement of the simulation results for the turbulent kinetic energy (Fig. 5 and 6) is also found to be better in "F2" flame. Similarly to the mean velocity in both two configurations the turbulent kinetic energy is better captured by means of the SMC based model. The concentrations of the main products of methane combustion, mass fractions of CO_2 (Fig. 7 and 8) and H_2O (Fig. 9 and 10), are predicted well with slight discrepancy on the outer side of the jet. It may be probably caused by the simplicity of the equilibrium chemistry model used. However, the measured results should be considered more carefully. Indeed it is a well known fact that the CO_2 concentration directly correlates to the temperature in hydrocarbon flames. The Fig. 3 and 4 show that the maximal mean temperature is still less than its adiabatic value that is also very good reproduced by the model. It is, therefore, surprising that CO_2 can reach such a high level at the same spatial locations in measurements. The same remark can be made on the prediction of H_2O mass fraction.

CONCLUSION

To summarize, it clearly appears that the proposed closure can be successfully applied in the technically relevant distributed reaction zone regime of combustion diagram (Peters 2000) if the fractal dimension depends on the Reynolds number. It is confirmed by the simulation results of two flames at different Reynolds numbers located in the distributed reaction zone regime. How the dependency of the fractal dimension on the local turbulent quantities can be formulated is still open. The experimental investigations on this subject are necessary and would be appreciated. The second but also important fact is that the combination of the proposed combustion model with the complete second order closures for the velocity and single reactive scalar correlations performs well and provides the most accurate results in predicting flow properties and species distribution in partially premixed flames.

Acknowledgment

The authors are very grateful to the Collaborative Research Centre SFB 568: Flow and Combustion in Future Gas Turbine Combustion Chambers (Germany) through the projects A4, B1 and D3 for the financial support.

REFERENCES

K. N. C. Bray and P. A. Libby: In P. A. Libby and F. A. Williams, editors, *Turbulent Reacting Flows*, pp. 309-374. Academic Press, London, San Diego, New York, 1994.

Y. C. Chen, N. Peters, G. A. Schneemann, N. Wruck, U. Renz, M. S. Mansour: The detailed flame structure of highly stretched turbulent premixed methane-air flames. *Combustion and Flame*, 107: pp. 223-244, 1996

F. C. Gouldin: An application of fractals to modelling premixed turbulent flames. *Comb. And Flame*, 68: pp. 249-266, 1987

W. P. Jones and B. E. Launder: The prediction of laminarization with a two equation model of turbulence. *Int. J. Heat Mass Transfer*, 15: pp. 301-314, 1972

B. E. Launder, G. C. Reece and W. Rodi: Progress in the development of a Reynolds-stress turbulence closure. *J. Fluid Mech.*, 68: pp. 537-566, 1975

B. E. Launder and S. Samaraweera: Application of a second moment turbulent closure to heat and mass transport in thin shear flows. *Int. J. Heat Mass Transfer*, 26: p 1631, 1979

C. K. Law: In N. Peters and B. Rogg: *Reduced Kinetic Mechanisms for Applications in Combustion Systems*, pp. 15-26. Springer-Verlag Berlin-Heidelberg. 1993

R. P. Lindstedt and E. M. Vaos: Modeling of premixed turbulent flames with second moment models. *Combustion and Flame*, 116: pp. 461-485, 1999

A. Maltsev, A. Sadiki and J. Janicka: Numerical prediction of partially premixed flames based on extended BML model coupled with mixing transport and ILDM chemical model, to be published in *ASME Turbo Expo 2003 Conference Proceedings*, June 16-19, 2003, Atlanta, Georgia, USA

B. B. Mandelbrot: On the geometry of homogeneous turbulence, with stress on the fractal dimension of the isosurfaces of scalars. *J. Fluid Mech.*, 72(2), pp. 401-416

N. Peters: *Turbulent Combustion*, Cambridge University Press, 2000

C. C. Shir: A preliminary study of atmospheric turbulent flows in the idealized planetary boundary layer. *J. Atm. Sci.*, 30: pp. 1327-1339, 1973

K. R. Sreenivasan: On the scaling of the turbulence energy dissipation rate. *Phys. Fluids*, 27(5): pp. 1048-1051, 1984

K. R. Sreenivasan and C. Meneveau: The fractal facets of turbulence. *J. Fluid Mech.*, 173: pp. 357-386, 1986

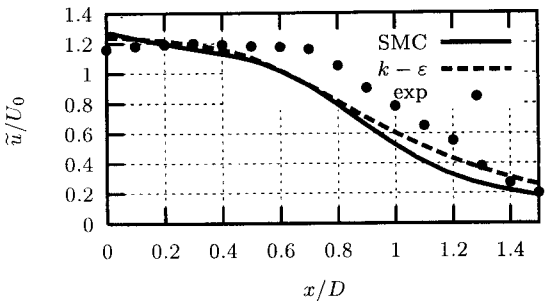

Fig. 1: F3. Axial velocity at $x/D = 8.5$

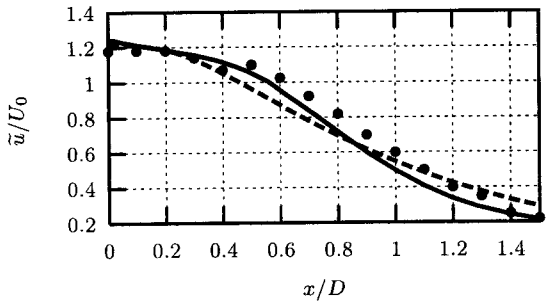

Fig. 2: F2. Axial velocity at $x/D = 10.5$

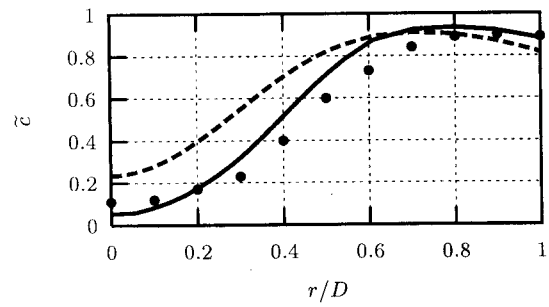

Fig. 3: F3. Single reactive scalar at $x/D = 8.5$

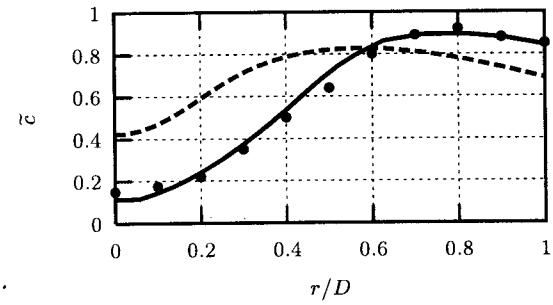

Fig. 4: F2. Single reactive scalar at $x/D = 10.5$

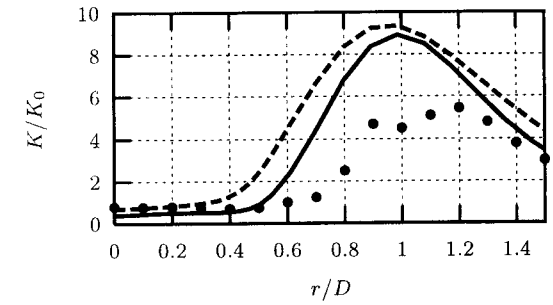

Fig. 5: F3. Turbulent kinetic energy at $x/D = 8.5$

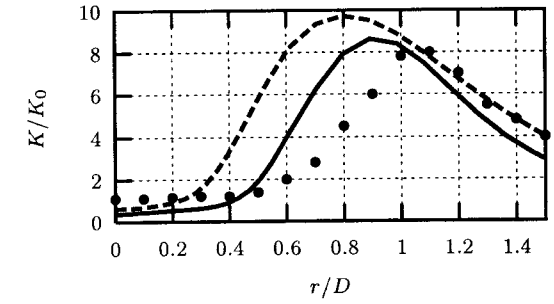

Fig. 6: F2. Turbulent kinetic energy at $x/D = 10.5$

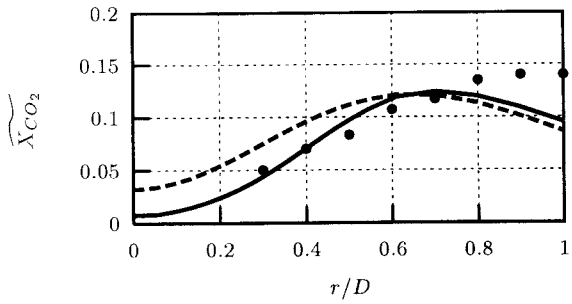

Fig. 7: F3. CO_2 mass fraction at $x/D = 8.5$

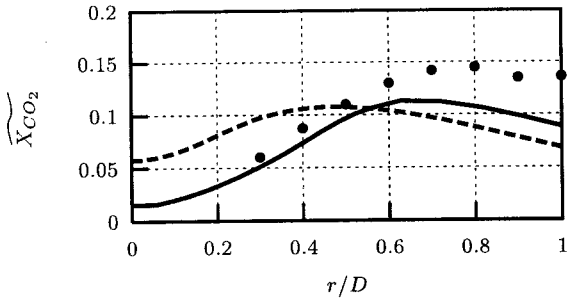

Fig. 8: F2. CO_2 mass fraction at $x/D = 10.5$

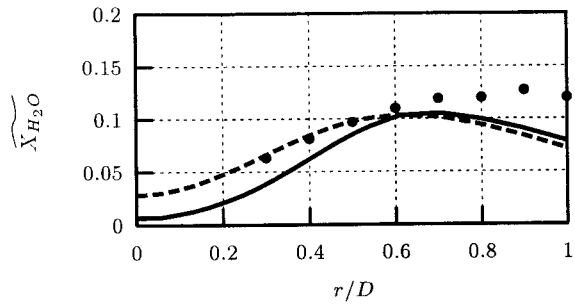

Fig. 9: F3. H_2O mass fraction at $x/D = 8.5$

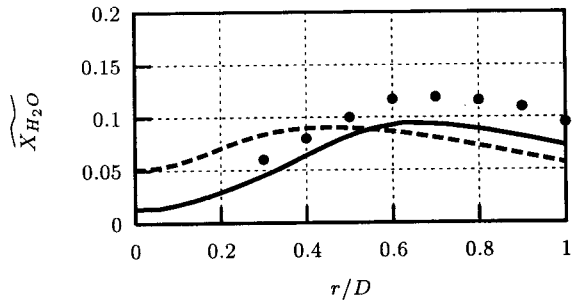

Fig. 10: F2. H_2O mass fraction at $x/D = 10.5$